

## Supporting Information

### **Construction of MAPbBr<sub>3</sub>/La<sub>2</sub>Ti<sub>2</sub>O<sub>7</sub> organic–inorganic dual perovskite heterojunction for photocatalytic CO<sub>2</sub> reduction**

<sup>a</sup>School of Food Science and Engineering, Changchun University, Changchun, 130022, China

<sup>b</sup>School of Materials Science and Engineering, University of Jinan, Jinan 250022, China.

Email: mse\_lik@ujn.edu.cn.

# 1. Experimental Section

## 1.1 Materials

Methylammonium bromide (MABr, 99.5%, CAS 6876-37-5), Lead bromide ( $\text{PbBr}_2$ , 99.0%, CAS 10031-22-8), Iron chloride hexahydrate ( $\text{FeCl}_3 \cdot 6\text{H}_2\text{O}$ , 98%, CAS 10025-77-1), Lanthanum nitrate hexahydrate ( $\text{La}(\text{NO}_3)_3 \cdot 6\text{H}_2\text{O}$ , 99%, CAS 10277-43-7), Sodium Hydroxide (NaOH, 97%, CAS 1310-73-2) were purchased from Shanghai Macklin Biochemical Co., Ltd. Titanic sulfate ( $\text{Ti}(\text{SO}_4)_2$ , 25-28%, CAS 13693-11-3), Isopropyl alcohol (99.5%, CAS 67-63-0) were purchased from Tianjin Fuyu Fine Chemical Co., Ltd. All chemicals were used without further purification. All of the reagents and solvents were commercially available and could be used without further purification.

## 1.2 Synthesis of $\text{MAPbBr}_3$

$\text{MAPbBr}_3$  nanocrystals were prepared by high-energy ball milling method.<sup>1</sup> MABr and  $\text{PbBr}_2$  were weighed with a molar ratio of 1 : 1, and then uniformly dispersed in 3 mL Isopropyl alcohol (IPA) by ultrasonic. Where the IPA acting as a grinding agent, would achieve sufficient grinding. The mixture was then transferred into a 25 mL agate grinding jar containing 5 agate grinding balls, and ground for 120 min at 600 rpm in a glove box under  $\text{N}_2$  atmosphere. After ball milling, the orange-yellow perovskite paste was centrifuged and washed with IPA for more than three times to remove unreacted substances, followed by vacuum drying at 60 °C overnight to obtain orange-yellow  $\text{MAPbBr}_3$  powder.

## 1.3 Synthesis of $\text{La}_2\text{Ti}_2\text{O}_7$ nanosheets

Briefly, 1.73 g  $\text{La}(\text{NO}_3)_3 \cdot 6\text{H}_2\text{O}$ , 1.61 g  $\text{Ti}(\text{SO}_4)_2$  were dissolved in 20 mL distilled water to form solution A, and 3.2 g NaOH in 40 mL distilled water was denoted as solution B. Solution B was added dropwisely into solution under stirring for 4 h, and then transferred into an 80 mL para-polyphenylene stainless-steel autoclave at 200 °C

for 24 h. The final products were treated and washed with 0.1 mol/L nitric acid and distilled water and finally dried at 60 °C.

#### *1.4 Synthesis of MAPbBr<sub>3</sub>/La<sub>2</sub>Ti<sub>2</sub>O<sub>7</sub>*

The synthesis of MAPbBr<sub>3</sub>/La<sub>2</sub>Ti<sub>2</sub>O<sub>7</sub> was similar to that of MAPbBr<sub>3</sub>, the only difference was the introduction of different amount of pre-synthesized LTO nanosheet.

#### *1.5 Materials Characterization*

The phase composition of samples was obtained by X-ray diffraction (XRD, D8 Advance) equipped with Cu K $\alpha$  radiation ( $\lambda = 1.54060 \text{ \AA}$ ). Fourier transform infrared spectroscopy (FT-IR) was collected on a Thermo Scientific Nicolet iS10 spectrometer. The morphologies and compositions of samples were observed on field emission scanning electron microscope (SEM, Gemini300) and transmission electron microscopy (TEM, JEM-2100Plus). The X-ray photoelectron spectroscopy (XPS) spectra were analyzed by a Thermo Fisher Scientific corporation Escalab 250Xi instrument. UV–vis DRS spectra was measured with Shimadzu UV-3600.

#### *1.6 Photocatalytic Experiments*

The photocatalytic CO<sub>2</sub> reduction performance was measured by a gas-solid test system under the visible light of 300W Xe lamp. The powder sample of 20 mg was weighed and placed on sample rack in a quartz reactor (100 ml) filled with CO<sub>2</sub> and water vapor. The vertical distance between the sample and the light source is maintained at 10 cm. 0.5 ml of deionized water is placed under the sample in the reactor to avoid direct contact with the sample. Subsequently, the sealed reactor is heated at 60 °C for 30 minutes to ensure that the deionized water becomes water vapor. During the test, the reactor temperature was controlled at 25 °C by a cooling circulating water machine. The water vapor participated in the chemical reaction as a proton source. 1 ml of gas product is extracted with a syringe every hour and analyzed by gas chromatography (GC-7900, CEAULight, China) with a TCD and FID detector.

### *1.7 Electrochemical measurements*

Photoelectrochemical characterizations were proceeded in Tetrabutylammonium hexafluorophosphate (TBAPF<sub>6</sub>) (0.1 M) solution with a standard three-electrode system on the electrochemical station (SP-150, Bio-Logic). The carbon cloth coated with catalyst, carbon rod and saturated Ag/AgCl were served as working electrode, counter electrode and reference electrode, respectively. Typically, a slurry of 4 mg of sample and 1 mL of ethanol were used to make the working electrode. The electrochemical impedance spectroscopy (EIS) was recorded from 0.01 Hz to 100 kHz with a sinusoidal ac perturbation of 10 mV. The impedance potential model was employed to collect the Mott-Schottky plots with the frequency of 500, 1000 and 2000 Hz. I-t curves were recorded using 300 W Xe lamp with a 420 nm cutoff filter.

## 2. Supporting Figures

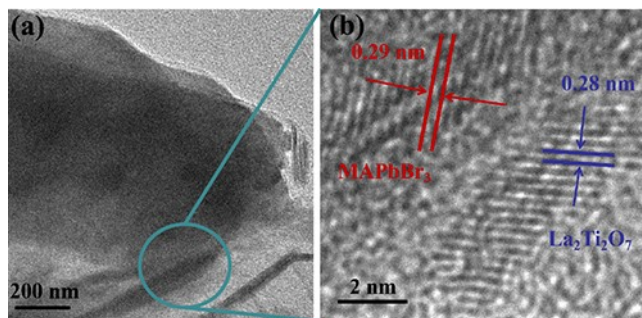


Fig. S1 (a) The transmission electron microscope (TEM) images of ML. (b) HRTEM images of ML.

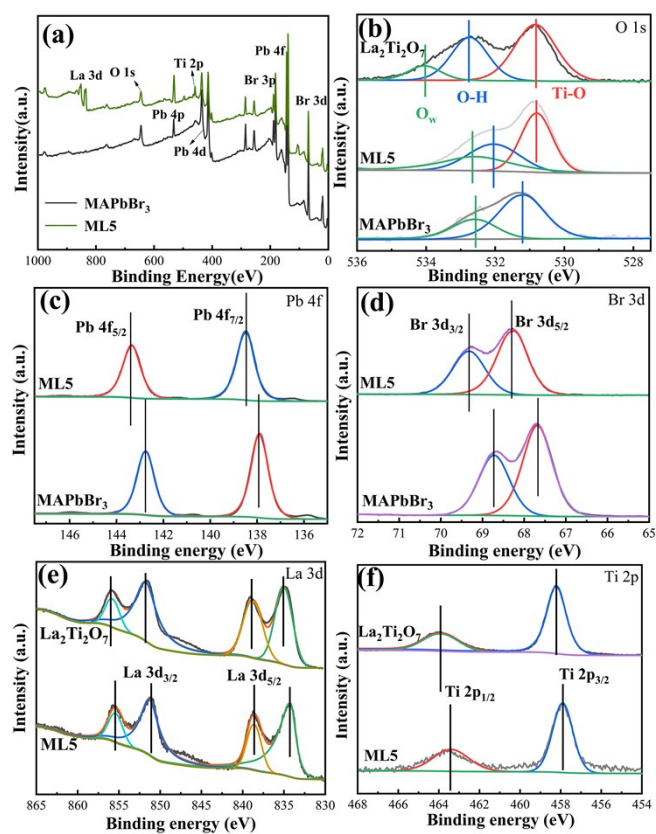


Fig. S2 XPS spectra of MAPbBr<sub>3</sub> and ML5: (a) survey spectra, (b) O 1s, (c) Pb 4f, (d) Br 3d; XPS spectra of La<sub>2</sub>Ti<sub>2</sub>O<sub>7</sub> and ML5: (e) La 3d, (f) Ti 2p.

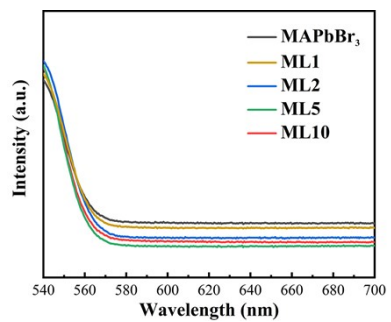


Fig. S3 UV-vis absorption spectra of MAPbBr<sub>3</sub> and MLs.

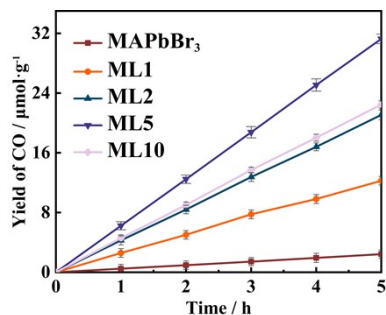


Fig. S4 The photocatalytic CO<sub>2</sub> reduction into CO for MAPbBr<sub>3</sub> and MAPbBr<sub>3</sub>/La<sub>2</sub>Ti<sub>2</sub>O<sub>7</sub>.

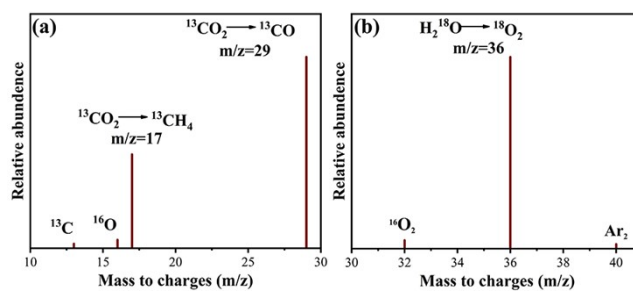


Fig. S5 Analysis of photocatalytic reduction of (a)  $^{13}\text{CO}_2$  and (b)  $^{18}\text{O}_2$  by Gas Chromatography Mass Spectrometry.

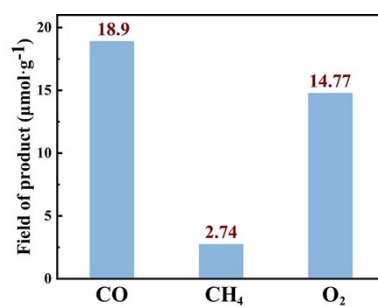


Fig. S6 The products of Photocatalytic CO<sub>2</sub> reduction

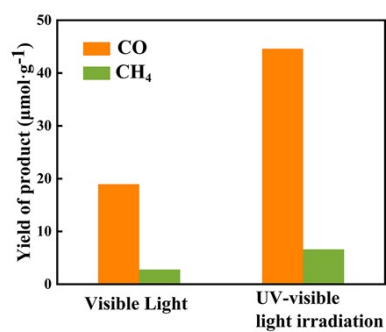


Fig. S7 Yield of photocatalytic CO<sub>2</sub> reduction under visible light and UV-visible light for three hours

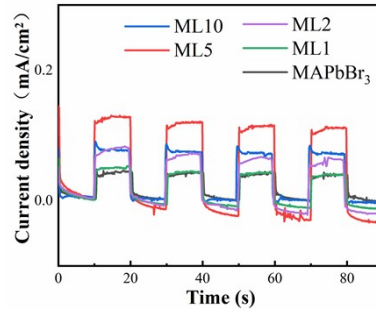


Fig. S8 The  $i-t$  curves and of MAPbBr<sub>3</sub>, La<sub>2</sub>Ti<sub>2</sub>O<sub>7</sub> and MAPbBr<sub>3</sub>/La<sub>2</sub>Ti<sub>2</sub>O<sub>7</sub>.

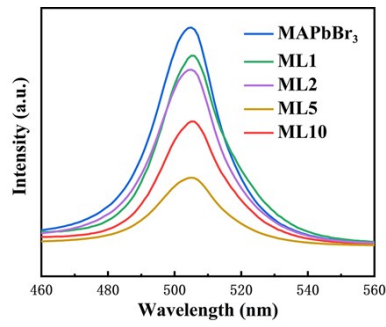


Fig. S9 Photoluminescence spectra of MAPbBr<sub>3</sub> and MLs.



### 3. Supporting Tables

Table S1 Resistance value (Rs and Rc) of MAPbBr<sub>3</sub>, La<sub>2</sub>Ti<sub>2</sub>O<sub>7</sub> and ML5.

Sample	Rs ( $\Omega$ )	Rc ( $\Omega$ )
MAPbBr <sub>3</sub>	12.17	21.33
ML5	3.58	6.19
La <sub>2</sub> Ti <sub>2</sub> O <sub>7</sub>	7.82	14.67

1. Y. Zhang, Y. Wang, X. Yang, L. Zhao, R. Su, J. Wu, D. Luo, S. Li, P. Chen, M. Yu, Q. Gong and R. Zhu, *Adv. Mater.*, 2021, **34**, 2107420.